Published in final edited form as:
Biomaterials. 2009 March ; 30(9): 1689–1696. doi:10.1016/j.biomaterials.2008.11.038.

Cells and Tissue Interactions with Glycated Collagen and their Relevance to Delayed Diabetic Wound Healing

Huijuan Liao, M.D./Ph.D.[1], **Julia Zakhaleva, M.D.**[2], and **Weiliam Chen, Ph.D., R.Ph.**[1,*]

1 *Department of Biomedical Engineering, State University of New York – Stony Brook, Health Science Center, Stony Brook, NY 11794-8181, USA*

2 *School of Medicine, State University of New York – Stony Brook, Health Science Center, Stony Brook, NY 11794-8191, USA*

Abstract

Dermal accumulation of advanced glycation end products (AGEs) has increasingly been implicated as the underlying cause of delayed diabetic wound healing. Devising an *in vitro* model to adequately mimic glycated tissues will facilitate investigation into the mechanism of glycation in conjunction with exploration of new approaches or improvement of current therapies for treating diabetic chronic wounds. Collagen matrices were artificially glycated and the presence of AGEs was demonstrated by immunostaining. Both the mechanical properties of the collagen matrices and their interactions with fibroblasts (morphology, attachment, proliferation, and migration) were altered after glycation, moreover, there was evidence of impairment on extracellular matrix (ECM) remodeling as well as inhibition of cell-induced material contraction. The actin cytoskeletons of the fibroblasts residing in the glycated collagen matrices were reorganized. *In vivo* mice full-thickness dermal wound models implanted with glycated collagen matrices showed delayed wound healing response. Thus, the glycated collagen matrix is an adequate *in vitro* model to mimic glycated tissues and could serve as a facile experimental tool to investigate the mechanism of glycation in conjunction with exploration of new approaches or improvement of current therapies for treating diabetic wounds.

Keywords

in vitro model; collagen matrix; glycation; fibroblast

1. Introduction

Protein glycation is initiated by spontaneous non-enzymatic reactions between free amino groups on long lived proteins and carbonyl groups of reducing sugars to form initially reversible Schiff bases, which subsequently undergo Amadori rearrangement leading to stable ketoamine bonds; these are generally referred to as advanced glycation end products (AGEs) [1]. The carboxymethyllysine (CML) structure is a prevalent AGE generated principally by oxidative cleavage of the Amadori intermediate [1,2]. Built-up of AGEs in dermis has increasingly been implicated as the underlying cause of delayed diabetic wound healing [3–5]. Clinical data

*Corresponding author. Tel: +1-631-444-2788. Fax: +1-631-444-6646. Email: weiliam.chen@stonybrook.edu.

compiled has hitherto demonstrated that accumulation of AGEs in extracellular matrix (ECM) is strongly correlated with the severity of diabetic wounds [6–13].

Preventative/reversal therapies for AGEs accumulation tested in either human clinical trials or animal studies have been shown to moderate development of diabetic wounds [14–17]. Nonetheless, the roles of AGEs in the pathogenesis of diabetes wounds have not yet been fully elucidated. Diabetic chronic wounds have recently been surgically addressed as implant-assisted healing with the goal of promoting tissue development in the wound beds; however, there is only a dearth of research into the interaction between these implants and diabetic wound beds that are presumably glycated. These were partly due to the lack of a credible and facile model suitable for performing experiments. Devising an *in vitro* model to adequately mimic glycated tissues will facilitate investigation into the mechanism of glycation in conjunction with exploration of new approaches or improvement of current therapies for treating diabetic wounds.

We aimed to take the initiative to develop and validate a facile glycation model suitable for *in vitro* investigation of cell-material interactions. Native collagen was used to construct this glycation model. Collagen is a well characterized natural material with multiple levels of structural order and it is a known substrate for cell attachment, growth and differentiation [18]. As a major component of dermal tissue, collagen has been incorporated into various implantable dermal substitutes with the goal of facilitating wound healing. In this study, lyophilized collagen matrices were modified by glyoxylic acid and their mechanical properties were evaluated. Primary mouse dermal fibroblast was utilized as a model cell type to evaluate the interactions with the glycated collagen matrix, which was followed by *in vivo* validation in a mouse transcutaneous dermal wound model. The results showed that glycation of collagen matrix modified its mechanical properties, altered cell-collagen interactions (both cell morphology and cell functions such as attachment, proliferation, migration), impaired ECM remodeling, inhibited fibroblast-mediated collagen contraction, and reorganized actin cytoskeleton as well as delayed wound closure and decreased cell recruitment in mouse full-thickness dermal wound model.

2. Materials and Methods

Commerically available lyophilized collagen matrices (DuraGen™) were manufactured by Integra Life Sciences (Plainsboro, NJ); this product has been extensively deployed clinically and utilized in pathological studies [19–22].

2.1 Glycation of Collagen Matrix

Following a similar procedure described previously [23–25], collagen matrices (weight: 50 mg each) were incubated for 24 h at 37°C in a solution of glyoxylic acid (0.715 g) and sodium cyanoborohydride (1.42 g), co-dissolved in sterile PBS (pH 7.8, 25 ml). Collagen matrices without glycation were used as controls. After treatment, all samples were exhaustively washed with distilled water.

2.2 Verification of Glycation in Collagen Matrix

The extent of collagen glycation was determined by immunofluorescence staining. Briefly, all samples were first incubated with a solution of anti-CML mouse monoclonal antibody (10 μg/ml, Cyclex, Nagano, Japan) for 1 h; this was followed by incubating them with a solution of goat anti-mouse FITC-labeled anti-IgG (34 μg/ml, Sigma-Aldrich, Saint Louis MO) for 30 min. Samples were then rinsed by three consecutive 5-minute washes with PBS. Control staining was performed by omitting anti-CML mouse monoclonal antibody. Glycation of the

collagen matrices were qualitatively assessed by examining for CML fluorescence under a laser scanning confocal microscope (LSCM, Zeiss LSM 510, Heidenheim, Germany).

2.3 Mechanical Property of Glycated Collagen Matrix

All experiments were carried out at ambient temperature. Each sample was uniaxially stretched by a modified Instron 4442 tensile tester (Instron Inc., Norwood, MA), where symmetrical deformation was carried out. The initial length between the Instron jaws was 30 mm and the stretching rate was set at 5 mm/min. Stress was calculated by dividing the force generated during stretching by the initial cross-sectional area, and strain was calculated as the ratio of the change in length in reference to the original sample length. All tests were performed in triplicate (n=3 per group).

2.4 Cell Isolation and Culture

Skins were obtained from the dorsal side of male mice (6 weeks, Balb/cj strain, Jackson Lab, Bar Harbor, ME) and primary fibroblasts were extracted by enzymatic digestion of the skin samples as described previously [26]. Briefly, the epidermis and dermis were separated by treating the skin with a 0.25% trypsin for 16 h at 4 °C. The dermis was digested with a collagenase type solution (2 mg/ml) (Gibco, Grand Island, NY), for overnight at 37 °C. Isolated fibroblasts were cultured in DMEM (Gibco, Grand Island, NY) supplemented with 10% fetal bovine serum (Hyclone, Logan, UT) and 1% Penicillin-Streptomycin solution (Gibco Grand Island, NY) at 37°C under a humidified atmosphere of 5% CO_2/95% air. Passages two to five were used for the following experiments and the cell culture media were changed every other day. Five hundred microliters of cell suspension (1×10^4 cells/well) was deposited into each well of a 24-well cell culture plate where either non-glycated collagen matrices or glycated collagen matrices (dimension: 10 mm diameter×1 mm thick) were pre-positioned. Collagen matrices with no cell seeded were used as negative controls. After incubated for 4 h, all samples were rinsed with PBS twice and transferred to a new 24-well plate containing fresh cell culture media. All studies were performed in triplicate (n=3 per group).

2.5 Cell Morphology, Viability, Migration and Distribution in Glycated Collagen Matrix

Briefly, fibroblasts-laden collagen matrices were retrieved 7 days after cell seeding, rinsed with PBS, incubated in 400 μl of "Live/Dead™" dye solution (Live/dead viability/cytotoxicity kit for mammalian cells, Molecular probe, Inc., Eugene, OR) containing a solution of 2 μM calcein AM (staining of live cells) and 4 μM EthD-1 (staining of dead cells) in PBS for 10 min at ambient temperature [27]. Cell morphology, viability, migration and spatial distribution were assessed under a LSCM. Random areas on every sample were selected for scanning and each area was progressively observed, profiled and analyzed in its entirety beginning from the surface at 2 μm increments. Digital planar images (along the X-Y plane) were captured incrementally along the depth (Z-axis) of the sample; cell densities and the distribution patterns of live (green) and dead (red) cells could be determined layer by layer. Tomographic reconstruction of 3D images and measurement of cell migration depth were conducted by Zeiss LSM 510 META software.

2.6 Cell Attachment and Proliferation in Glycated Collagen Matrix

For quantification of cell attachment and proliferation, a colorimetric MTS assay (CellTiter 96® AQueous One Solution Cell Proliferation Assay kit, Promega, Madison, WI) was performed at 4 h (attachment phase) and 3 days, and 1, 2, 3 and 4 weeks (proliferation phase) after cell seeding [27]. The collagen matrices were removed from the original culture, rinsed with PBS followed by incubation with a 20% MTS reagent in serum-free culture media for 1 h. Two hundred microliters of the media from each well were transferred to a 96-well plate

and the optical density (OD, absorbance: 490 nm) was determined by a microplate reader (Infinite 200, Tecan; Switzerland).

2.7 ECM Deposition in Glycated Collagen Matrix

After 7 days in culture, samples were retrieved and rinsed twice with PBS; this was followed by fixation in 70% ethanol for 10 min. Verhoeff staining kit (Electron Microscopy Sciences, Fort Washington, PA) was utilized to detect the presence of elastin. Briefly, the fixed samples were immersed in Verhoeff solution for 7 min followed by rinsing with tap water for 1 min for removal of unbound dye [28].

ECM production by cells inside the collagen matrices was visualized using fibronectin as a surrogate through immunofluorescent staining. Briefly, samples were first fixed with 4% paraformaldehyde and permeabilized with 0.01% TritonX-100; they were blocked with a 1% BSA in PBS before adding the primary antibody. Samples were incubated with mouse monoclonal anti-fibronectin antibody (Sigma-Aldrich, Saint Louis, MO) (diluted in PBS at 1:100) for 3 hours at room temperature. After three consecutive 5-minute washes with PBS, goat anti-mouse FITC-labeled anti-IgG (Sigma-Aldrich, Saint Louis, Missouri, MO) was applied and incubated for 30 min. Cell nuclei were visualized by counterstaining with 4′, 6-diamino-2-phenylindol-dihydrochloride, DAPI (1 μg/mL). Control staining was performed by omitting the primary antibodies. Images of Verhoeff stained and fibronectin immunofluorescent stained samples were captured by LSCM and under conventional light microscopy, respectively.

2.8 Fibroblast Induced Contraction of Glycated Collagen Matrix

After incubating for the time-spans ranging from 0 days to 4 weeks, cell-laden collagen matrices were retrieved at various time-points, their diameters were measured with an electronic digital caliper (Jed Pella, Inc., Redding, CA).

2.9 Actin Cytoskeleton Organization in Glycated Collagen Matrices

Cells residing in collagen matrices were stained with the F-actin probe phalloidin as previously described [28]. Briefly, the collagen matrices were first fixed in a 4% paraformaldehyde solution, permeabilized with a 0.01% TritonX-100, followed by incubation with Alexa Fluor 546 Phalloidin (ex: 556 nm, em: 573 nm) for 15 min at ambient temperature. Cell nuclei were counterstained with DAPI. Cell cytoskeleton organizations were imaged by LCSM.

2.10 Implantation of Glycated Collagen Matrix in a Mouse Full-thickness Dermal Wound Model

All animal studies were performed in compliance with the guidelines prescribed by the Institutional Animal Care and Use Committee of SUNY-Stony Brook (IACUC Protocol # 2006-1320). Male mice (6 weeks, Balb/cj strain, Jackson Lab, Bar Harbor, ME) were anesthesized with isoflurane (5% for induction and 2.5 to 3% for maintenance). After removal of the hair on their dorsal side, a full-thickness excisional wound was surgically created (approximate diameter: 1 cm) on each mouse. Collagen matrices (glycated or non-glycated, n=5) were trimmed to approximate the size of the wound beds created and deposited directly into them. After implantation, each wound bed was covered by plastering Tegaderm™ over the entire wound surface and the adjoining intact tissue followed by a Band-Aid™. All animals were euthanized after 7 days of implantation. The extent of wound contraction was first determined by a digital caliper. Thereafter, intact wounds specimens were excised, preserved in formalin, paraffin-embedded, sectioned, stained with H&E, and examined by light microscopy. Cell recruitments in the collagen matrix were assessed by counting 10 random

sectors in each wound beds for the presence of recruited cells and calculated by dividing cell number by observed space.

2.11 Statistics

Statistical comparisons between groups of samples were analyzed using *t*-test. Values are cited as mean ± standard deviation. $p<0.05$ was taken as significant.

3. Results and discussion

3.1 Formation of Glycation in Collagen Matrix

The matrix structure remained intact in both glycated and non-glycated collagen matrices. As shown in Fig. 1, glycation of virtually all collagen fibers was demonstrated by positive immunofluorescent staining with antibodies specific to CML. The glycated collagen matrix theoretically mimics the highly glycated condition of diabetic subjects as epitomized by the high levels of CMLs present in their skin.

3.2 Alteration of Mechanical Properties of Collagen Matrix by Glycation

The mechanical properties of both glycated and non-glycated collagen matrices as reflected by their stress-strain curves were depicted in Fig. 2. When compared to the non-glycated collagen matrices, the glycated collagen matrices exhibited a significant increase in both their Young's Moduli (0.054 GPa *vs.* 0.040 GPa, $p=0.042$) and the areas under the stress-strain curve (83.2 MJ/m^3 *vs.* 74.4 MJ/m^3, $p=0.038$). The direct implication was a decreased elasticity and increased toughness of the glycated collagen matrices, which paralleled the loss of elasticity in glycated collagenous tissues in diabetes subjects. Glycation altered the mechanical property of collagen fibers which ultimately translated into increased rigidity and brittleness of tissues, thus compromising their functional roles.

3.3 Cell Morphology, Attachment, Proliferation, Migration and Their 3D Distribution in Glycated Collagen Matrix

Cell-laden collagen matrices were stained with Live/dead™ dye, subjected to LSCM and the digitized images captured were assembled into 3D images via tomographic reconstruction. Cell attachment and their long-term viability and proliferation in the glycated collagen matrices were quantified directly by performing MTS assay. In general (Fig. 3), cells adhered to both the glycated collagen and non-glycated collagen matrices 4 h after seeding; proliferation occurred during subsequent incubation with cell migration depth increased with incubation time. The overwhelming majority (> 95%) of the cells were alive with no noticeable difference in cell distribution patterns. However, as shown in Fig 3A, attachment of fibroblasts was clearly compromised in the glycated collagen matrix; the cell numbers (OD: 0.337 ± 0.003) at 4 hours were significantly less than its non-glycated counterpart (OD: 0.554 ± 0.007, $p=0.029$). Compared with the non-glycated collagen matrix, the increments of cell number in the glycated collagen matrix were significantly lower (OD: 3.694 ± 0.140 *vs.* 4.517 ± 0.147, $p=0.001$) and it took considerably longer for cells to reach a proliferative plateau phase compared with incubating cells in the non-glycated collagen matrix (3 weeks *vs.* 2 weeks); moreover, the peak cell number and cell migration depth (Fig. 3B) were both considerably lower (OD: 4.031 ± 0.140 *vs.* 5.050 ± 0.239, $p=0.037$; depth: 105 ± 7 *vs.* 130 ± 7 μm, $p=0.001$). Cells residing in the glycated collagen matrix (Fig. 3C) typically assumed less spread out conformations as compared to those residing inside the non-glycated collagen matrix (Fig. 3D). Once thought to solely provide mechanical functions, collagen fibers are now recognized to play critical roles in regulation of cell attachment, cell migration, in conjunction with stimulating and controlling their development and growth. Evidently, modification of collagen through glycation compromised its physiological functions; this was exemplified by our results showing that the

glycated collagen had produced modification of cell morphologies and functions such as attachment, proliferation, and migration. In diabetic wounds, compromise of ECM function due to glycation is manifested by a decreased fibroblast population, which leads to reduced granulation tissue volume and delayed re-epithelialization [29]. Cells interact with collagen through integrins via specific amino acid sequences along the collagen molecule. Glycation resulted in both structural and charge modification of collagen, thereby impeding cell-collagen interaction. This was consistent with the previously published data showing modification of arginine side-chains of collagen resulted in a reduction of cell adhesion and spreading [30].

3.4 ECM Remodelling in Glycated Collagen Matrix

Both elastin and fibronectin are non-proteoglycan matrix components of ECM synthesized by fibroblasts. Fibroblasts-laden collagen matrices were stained for the presence of elastin and fibronectin by Verhoeff staining and immunofluorescent method, respectively. All the reagents utilized do not have affinity towards collagen. As shown in Fig. 4A-1 and 4B-1, the intensity of elastin staining and its distribution density in the glycated collagen matrix were both noticeably lower than those of their non-glycated counterparts. The results produced by immunofluorescent staining of fibronectin further corroborated and unveiled the ECM distribution profile visualized by Verhoeff staining. Evidently, the glycated collagen matrix (Fig. 4A-2) showed a less abundance of fibronectin surrounding the fibroblasts compared to the non-glycated collagen matrix (Fig. 4B-2). The imbalance of ECM homeostasis in a glycated collagen matrix bears a resemblance to diabetic chronic wound beds, which are generally accompanied by diminished ECM deposition [31]. It is possible that glycation of collagen matrix directly inhibits the synthesis and/or excretion of ECM via the interplay of AGEs and cellular receptors such as Receptor of AGE (RAGE), which are capable of stimulating cellular activation towards dysfunction and tissue destruction [13], alternatively, a mechanism through suppressing attachment, migration and proliferation of fibroblasts could result in decreasing of fibroblasts thus impeding ECM deposition. Fibroblasts are known to secrete a repertoire of hydrolases including matrix metalloproteinases (MMPs), which could degrade both the ECM and the collagen matrix. Decrease in susceptibility to MMPs via blockade of the enzymes' active sites, interference with ligand binding by crosslinking induced compaction of collagen fibers and alteration of ECM proteins' half-lives could all be contributory to the diminished deposition of ECM in the glycated collagen matrix [32]. In turn, impairment of ECM remodeling prohibits the migration and proliferation of fibroblasts [33]. Further investigation directing towards these aspects are ongoing.

3.5 Fibroblast Induced Contraction of Glycated Collagen Matrix

Fibroblasts residing on collagen exert forces on the collagen fibrils and, with time, leading to contraction of the collagen template, thus, reducing its overall surface area [34–36]. Collagen contraction is dependent on the dynamic activity of cells exerting traction forces on the collagen network with a reduction in the extent of its hydration similar to squeezing fluid from a soaked sponge. In this study, the effect of glycation on fibroblasts mediated contraction of the collagen matrix was determined. Reduced contractions in the glycated collagen matrices, compared with non-glycated collagen matrices, were observed throughout the entire course of the study with the magnitude noticeably greater after 1 weeks of incubation (Fig. 5). It should be noted that unlike fibroblast-laden collagen thin films (i.e., a 2D structure) which typically contracted strongly after 4 h of incubation and reached maximum within 24 h (data not shown), the 3D (~3.5 mm thick) collagen matrices were highly porous and thus structurally more robust, the discontinuous structure rendered it more resistant to traction force collectively generated by cells initially residing on/inside it after seeding. The continual increase in cell number in conjunction with their constant infiltration into the matrices with time eventually produced sufficient force and achieved full contraction of the 3D collagen matrices. These results combining with the findings summarized above emulate the clinical observation that increased

accumulation of AGEs in the tissues of diabetic subjects greatly affects the mechanical properties of collagen fibers and also impairs their resistance to proteolysis [6,37]. It could thus be inferred that reduction of fibroblast population, diminished ECM remodeling, increased resistance of glycated collagen to proteolysis and formation of a less deformable matrix are all causative factors of reduction in the contraction of the glycated collagen matrix.

3.6 Actin Cytoskeleton Organization in Glycated Collagen Matrix

Analyses of the pattern of fluorescent stained actin revealed that fibroblasts grown in glycated collagen matrices formed large and well-defined actin microfilaments (Fig. 6A), suggesting resistance of the glycated collagen matrices to contraction resulted in increased tension of the fibroblasts. In contrast, the fibroblasts residing in non-glycated collagen matrices have considerably fewer actin microfilaments (Fig. 6B); suggesting lesser resistance to forces and tension. Formation of large and dense bundles of actin microfilaments within the cells inside the glycated collagen matrices were likely due to the increased mechanical stress imparted by glycation. This study produced circumstantial evidence of the mechanistic basis for the alteration of mechanical property through glycation. Additionally, we also identified the presence of extensive connections formed among the actin microfilaments in the non-glycated collagen matrices, revealing robust contact between adjoining cells. Conversely, the connections of actin microfilaments amongst cells in the glycated collagen matrices were generally aloof or discontinued halfway. The direct implication of these impaired connections is either weakened or partially inhibited cellular signal communication, which could account for both the reduced cell numbers and impaired ECM remodeling observed in the glycated collagen matrices.

3.7 *In Vivo* Response to Glycated Collagen Matrix in a Mouse Full-thickness Dermal Wound Model

Dermal wound healing is a highly orchestrated complex sequence of interactive events comprising various cell types (e.g., macrophages, fibroblasts, keratinocytes, etc.) leading to eventual wound closure [38–40]. This process ordinarily starts as an inflammatory response mediated largely by macrophages, culminates in repair of the dermal injury through ECM deposition by fibroblasts with concomitant regeneration of a new epidermal layer by keratinocytes, thus, signifying wound closure [39]. In particular, timely and orderly infiltration of macrophages, migration/proliferation of dermal fibroblasts and likewise, keratinocytes are regarded as some of the key features of successful wound healing [33].

The gross appearances of the glycated collagen matrices explanted suggested that both the matrices and their degradation byproducts were non-cytotoxic. Lacking redness or edema adjoining the implants suggested the absence of extensive acute inflammatory responses, with no sign of tissue necrosis (not shown). Visual observation of the wound beds implanted with glycated collagen matrices showed signs of impaired healing. As shown in Fig. 7A, the averaged size of the wound beds implanted with glycated collagen matrices (7.8 ± 0.8 mm) was significantly larger than that of implanted with non-glycated collagen matrices (5.9 ± 0.5 mm, p=0.044); the latter appeared to have contracted with no evidence of fluid oozing when compared to the former. H&E stained histopathology sections of the wound beds were examined. Overall, fewer cells ($1.5 \pm 0.5\times10^4/mm^3$) were recruited to the interior of the glycated collagen matrices (Fig. 7C) as compared to their non-glycated counterparts ($3.7 \pm 0.8\times10^4/mm^3$, p=0.001) (Figure 7D); moreover, the extent of epidermal regeneration, manifested as epidermal hyperplasia/re-epithelialization, of the former were apparently lesser than the latter. This pattern of epidermal regeneration across the surfaces of collagen matrices was indeed consistent with the results obtained in our previous related *in vivo* investigation utilizing native collagen matrices in a similar model [41]. Analyses of these specimens at higher magnifications revealed that the majority of cells infiltrated deep into the collagen matrices

(i.e., away from the wound bed) were macrophages with an abundance of fibroblasts occupying the areas adjoining and in close proximity to the tissues.

Diabetic chronic wounds are characterized by delayed wound closure and to a large extent also epitomized by diminished cell recruitments and growth in conjunction with impaired migration/formation of the epidermis over the wounds [42]. We have observed the similarities of the biological responses towards the glycated collagen matrix, both *in vitro* and *in vivo*, which parallel multiple aspects of the typically observed clinical manifestations of chronic wounds. Thus, the glycated collagen matrix could serve as a facile *in vitro* model to investigate the interaction between cells and biomaterials. Future studies will be focused on further developing this glycation model using primary cells isolated from diabetic mice and culturing them in a high glucose environment in order to emulate diabetes.

4. Conclusions

The present study validates the feasibility of using a glyoxylic acid modified collagen matrix as a facile but adequate *in vitro* model to mimic glycated tissues. This model emulates the general clinical manifestations of diabetic wound healing and it could be deployed to study the interactive behaviors of cells and evaluate the performance of engineered implantables designed to enhance diabetic chronic wound healing. Lastly, it could also be utilized as an experimental tool for elucidating the pathological mechanisms of glycation and efficacy screenings for new therapeutic approaches designed to treat diabetic chronic wounds.

Acknowledgements

This study was supported by a grant from the National Institutes of Health (R01 DK068401). Partial supported was also provided by an Enhanced Center of Advanced Technology (ECAT) grant of the New York State Foundation for Science Technology and Innovation (NYSTAR) administered by the Center for Biotechnology. We gratefully thank Dr. Hongyang Ma for his assistance in performing the mechanical property testing, and Dr. Guowei Tian for his assistance in LSCM scans and image processing.

References

1. Ahmed N. Advanced glycation end products--role in pathology of diabetic complications. Diabetes Res Clin Pract 2005;67(1):3–21. [PubMed: 15620429]
2. Singh R, Barden A, Mori T, Beilin L. Advanced glycation end-products: a review. Diabetologia 2001;44(2):129–46. [PubMed: 11270668]
3. Brownlee M. Advanced protein glycosylation in diabetes and aging. Annu Rev Med 1995;46:223–34. [PubMed: 7598459]
4. Friedman EA. Advanced glycosylated end products and hyperglycemia in the pathogenesis of diabetic complications. Diabetes Care 1999;22(Suppl 2):B65–71. [PubMed: 10097902]
5. Ahmed MU, Brinkmann Frye E, Degenhardt TP, Thorpe SR, Baynes JW. N-epsilon-(carboxyethyl) lysine, a product of the chemical modification of proteins by methylglyoxal, increases with age in human lens proteins. Biochem J 1997;324(Pt 2):565–70. [PubMed: 9182719]
6. Monnier VM, Vishwanath V, Frank KE, Elmets CA, Dauchot P, Kohn RR. Relation between complications of type I diabetes mellitus and collagen-linked fluorescence. N Engl J Med 1986;314 (7):403–8. [PubMed: 3945267]
7. Vishwanath V, Frank KE, Elmets CA, Dauchot PJ, Monnier VM. Glycation of skin collagen in type I diabetes mellitus. Correlation with long-term complications. Diabetes 1986;35(8):916–21. [PubMed: 3732633]
8. Sell DR, Monnier VM. End-stage renal disease and diabetes catalyze the formation of a pentose-derived crosslink from aging human collagen. J Clin Invest 1990;85(2):380–4. [PubMed: 2298912]
9. Monnier VM, Sell DR, Nagaraj RH, Miyata S, Grandhee S, Odetti P, et al. Maillard reaction-mediated molecular damage to extracellular matrix and other tissue proteins in diabetes, aging, and uremia. Diabetes 1992;41(Suppl 2):36–41. [PubMed: 1526333]

10. Vasan S, Foiles P, Founds H. Therapeutic potential of breakers of advanced glycation end product-protein crosslinks. Arch Biochem Biophys 2003;419(1):89–96. [PubMed: 14568012]
11. Monnier VM, Sell DR. Prevention and repair of protein damage by the Maillard reaction in vivo. Rejuvenation Res 2006;9(2):264–73. [PubMed: 16706654]
12. Nicholls K, Mandel TE. Advanced glycosylation end-products in experimental murine diabetic nephropathy: effect of islet isografting and of aminoguanidine. Lab Invest 1989;60(4):486–91. [PubMed: 2496273]
13. Niu Y, Xie T, Ge K, Lin Y, Lu S. Effects of extracellular matrix glycosylation on proliferation and apoptosis of human dermal fibroblasts via the receptor for advanced glycosylated end products. Am J Dermatopathol 2008;30(4):344–51. [PubMed: 18645306]
14. Nilsson BO. Biological effects of aminoguanidine: an update. Inflamm Res 1999;48(10):509–15. [PubMed: 10563466]
15. Stracke H, Lindemann A, Federlin K. A benfotiamine-vitamin B combination in treatment of diabetic polyneuropathy. Exp Clin Endocrinol Diabetes 1996;104(4):311–6. [PubMed: 8886748]
16. Cameron NE, Cotter MA, Dines K, Love A. Effects of aminoguanidine on peripheral nerve function and polyol pathway metabolites in streptozotocin-diabetic rats. Diabetologia 1992;35(10):946–50. [PubMed: 1451951]
17. Dorrian CA, Cathcart S, Clausen J, Shapiro D, Dominiczak MH. Factors in human serum interfere with the measurement of advanced glycation endproducts. Cell Mol Biol (Noisy-le-grand) 1998;44 (7):1069–79. [PubMed: 9846889]
18. Ruszczak Z. Effect of collagen matrices on dermal wound healing. Adv Drug Deliv Rev 2003;55(12): 1595–611. [PubMed: 14623403]
19. McCall TD, Fults DW, Schmidt RH. Use of resorbable collagen dural substitutes in the presence of cranial and spinal infections-report of 3 cases. Surg Neurol 2008;70(1):92–6. [PubMed: 18262619]
20. Grigoryants V, Jane JA Jr, Lin KY. Salvage of a complicated myelomeningocele using collagen (Duragen) and dermal (Alloderm) matrix substitutes. Case report and review of the literature. Pediatr Neurosurg 2007;43(6):512–5. [PubMed: 17992043]
21. Zerris VA, James KS, Roberts JB, Bell E, Heilman CB. Repair of the dura mater with processed collagen devices. J Biomed Mater Res B Appl Biomater 2007;83(2):580–8. [PubMed: 17465025]
22. Narotam PK, José S, Nathoo N, Taylon C, Vora Y. Collagen matrix (DuraGen) in dural repair: analysis of a new modified technique. Spine 2004;29(24):2861–7. [PubMed: 15599291]discussion 2868–9
23. Alikhani Z, Alikhani M, Boyd CM, Nagao K, Trackman PC, Graves DT. Advanced glycation end products enhance expression of pro-apoptotic genes and stimulate fibroblast apoptosis through cytoplasmic and mitochondrial pathways. J Biol Chem 2005;280(13):12087–95. [PubMed: 15590648]
24. Kislinger T, Fu C, Huber B, Qu W, Taguchi A, Du Yan S, et al. N(epsilon)-(carboxymethyl)lysine adducts of proteins are ligands for receptor for advanced glycation end products that activate cell signaling pathways and modulate gene expression. J Biol Chem 1999;274(44):31740–9. [PubMed: 10531386]
25. Santana RB, Xu L, Chase HB, Amar S, Graves DT, Trackman PC. A role for advanced glycation end products in diminished bone healing in type 1 diabetes. Diabetes 2003;52(6):1502–10. [PubMed: 12765963]
26. Ng KW, Khor HL, Hutmacher DW. *In vitro* characterization of natural and synthetic dermal matrices cultured with human dermal fibroblasts. Biomaterials 2004;25(14):2807–18. [PubMed: 14962559]
27. Weng L, Pan H, Chen W. Self-crosslinkable hydrogels composed of partially oxidized hyaluronan and gelatin: *in vitro* and *in vivo* responses. J Biomed Mater Res A 2008;85(2):352–65. [PubMed: 17688243]
28. Pan H, Jiang H, Chen W. Interaction of dermal fibroblasts with electrospun composite polymer scaffolds prepared from dextran and poly lactide-co-glycolide. Biomaterials 2006;27(17):3209–20. [PubMed: 16499965]
29. Vande Berg JS, Robson MC, Mikhail RJ. Extension of the life span of pressure ulcer fibroblasts with recombinant human interleukin-1 beta. Am J Pathol 1995;146(5):1273–82. [PubMed: 7747819]
30. Paul RG, Bailey AJ. The effect of advanced glycation end-product formation upon cell-matrix interaction. Int J Biochem Cell Biol 1999;31(6):653–60. [PubMed: 10404638]

31. Fuji A, Kobayashi S, Yamamoto H, Tamura T. Augmentation of wound healing by royal jelly (RJ) in streptozotocin-diabetic rats. Jpn J Pharmacol 1990;53(3):331–7. [PubMed: 2391765]
32. Vlassara H, Palace MR. Diabetes and advanced glycation end products. J Intern Med 2002;251(2): 87–101. [PubMed: 11905595]
33. Desmoulière A, Gabbiani G. Modulation of fibroblastic cytoskeletal features during pathological situations: The role of extracellular matrix and cytokines. Cell Motil Cytoskeleton 1994;29(3):195–203. [PubMed: 7895283]
34. Tomasek JJ, Akiyama SK. Fibroblast-mediated collagen gel contraction does not require fibronectin-alpha 5 beta 1 integrin interaction. Anat Rec 1992;234(2):153–60. [PubMed: 1416102]
35. Bell E, Ivarsson B, Merrill C. Production of a tissue-like structure by contraction of collagen lattices by human fibroblasts of different proliferative potential *in vitro*. Proc Natl Acad Sci U S A 1979;76 (3):1274–8. [PubMed: 286310]
36. Gullberg D, Tingström A, Thuresson AC, Olsson L, Terracio L, Borg TK, et al. Beta 1 integrin-mediated collagen gel contraction is stimulated by PDGF. Exp Cell Res 1990;186(2):264–72. [PubMed: 2298242]
37. Reiser KM. Nonenzymatic glycation of collagen in aging and diabetes. Proc Soc Exp Biol Med 1998;218(1):23–37. [PubMed: 9572149]
38. Singer AJ, Clark RA. Cutaneous wound healing. N Engl J Med 1999;341(10):738–46. [PubMed: 10471461]
39. Blakytny R, Jude E. The molecular biology of chronic wounds and delayed healing in diabetes. Diabet Med 2006;23(6):594–608. [PubMed: 16759300]
40. Chettibi, S.; Ferguson, MWJ. Wound repair: an overview. In: Gallin, JI.; Snyderman, R., editors. Inflammation: Basic Principles and Clinical Correlates. Vol. 3. Philadelphia: Lippincott. Williams and Wilkins; 1999. p. 865-81.
41. Wang Z, Pan H, Yuan Z, Liu J, Chen W, Pan Y. Assessment of dermal wound repair after collagen implantation with optical coherence tomography. Tissue Eng Part C Methods 2008;14(1):35–45. [PubMed: 18454644]
42. Loots MA, Lamme EN, Zeegelaar J, Mekkes JR, Bos JD, Middelkoop E. Differences in cellular infiltrate and extracellular matrix of chronic diabetic and venous ulcers versus acute wounds. J Invest Dermatol 1998;111(5):850–7. [PubMed: 9804349]

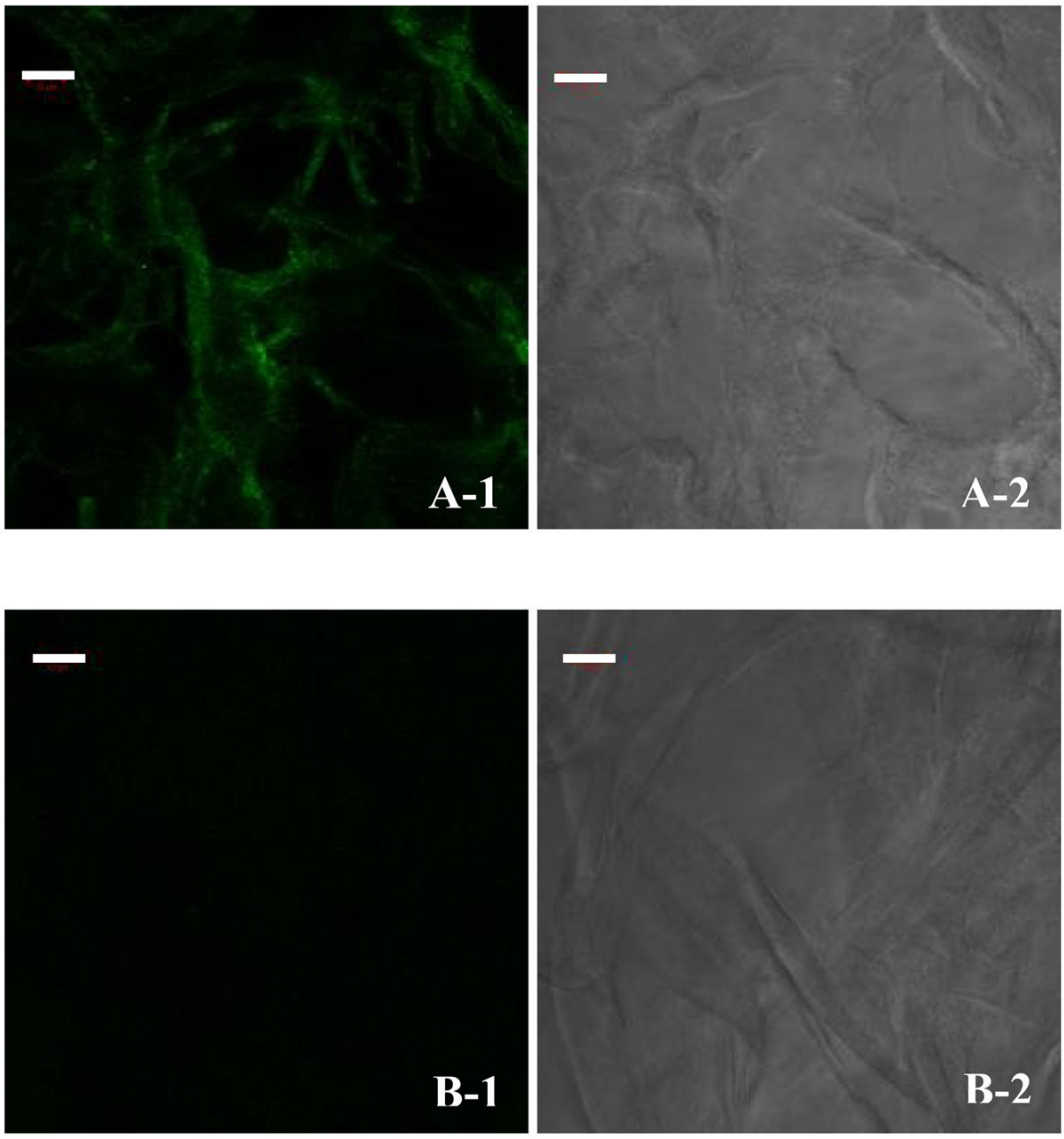

Fig. 1.
Immunofluorescence staining for the presence of CML in, (A) a glycated collagen matrix, and (B) a non-glycated collagen matrix. (A-1 and B-1) fluorescent, and (A-2 and B-2) phase contrast. Scale bar: 50 μm.

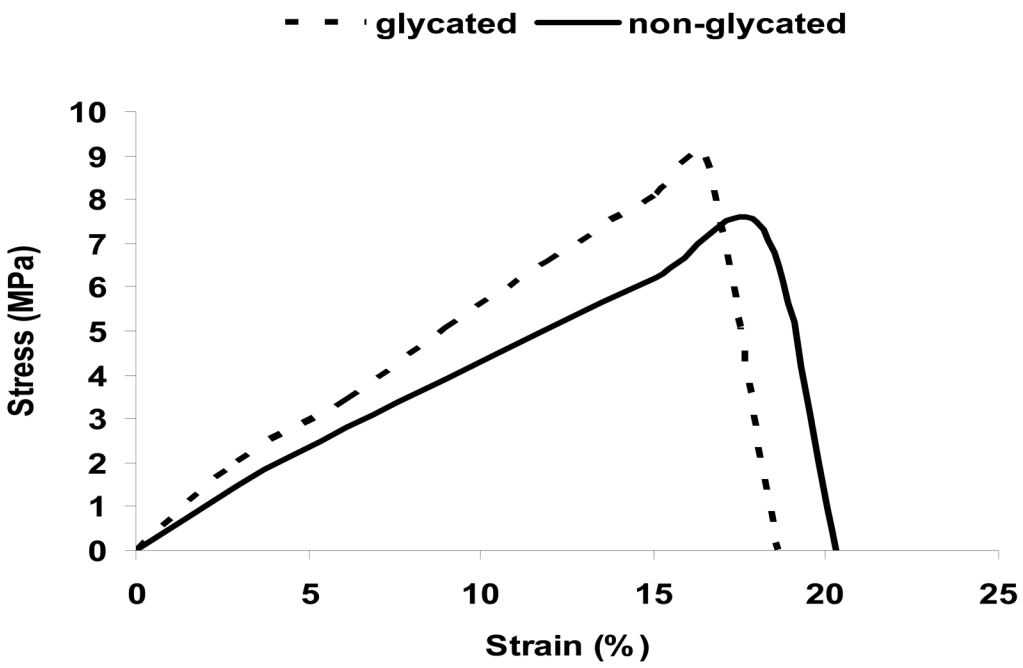

Fig. 2.
Stress-strain curves of glycated and non-glycated collagen matrices.

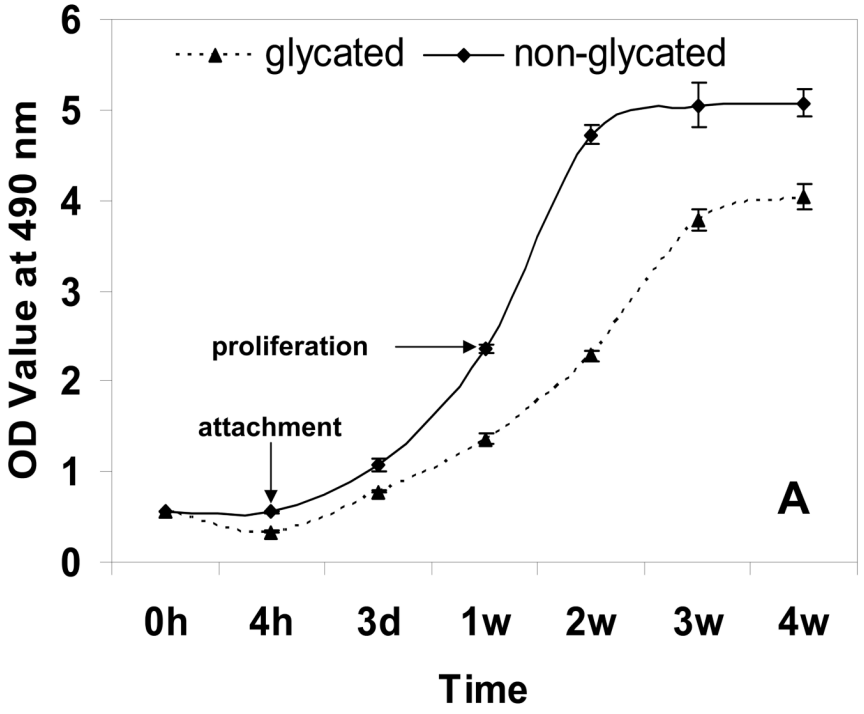

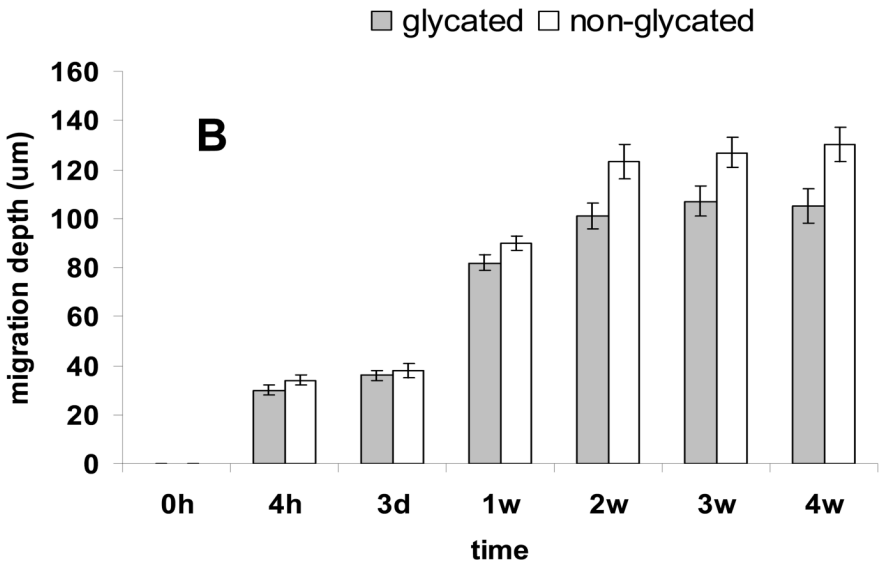

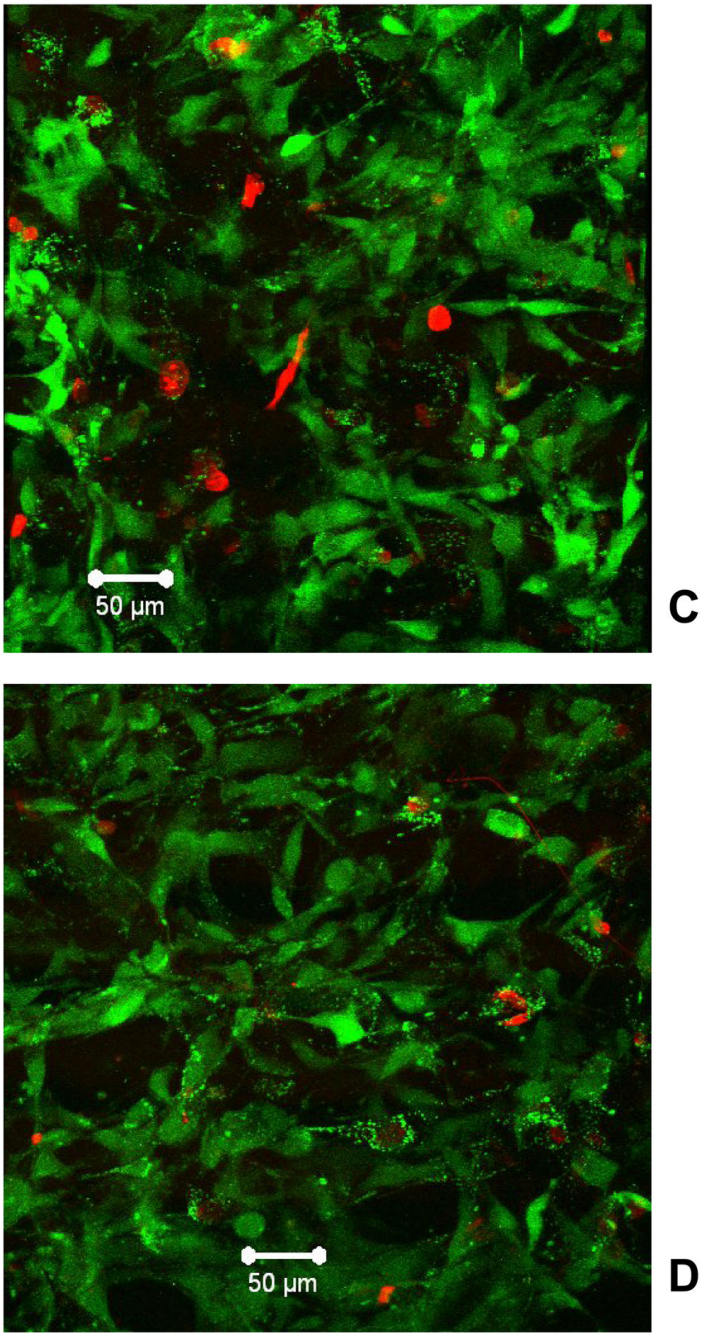

Fig. 3.
Fibroblasts population and distribution in collagen matrices. (A) MTS assay for cell proliferation, (B) cell migration depth inside matrices, (C) spatial distribution of cells in a glycated collagen matrix, and (D) spatial distribution of cells in a non-glycated collagen matrix. Green: live cells; red: dead cells. Scale bar: 50 μm.

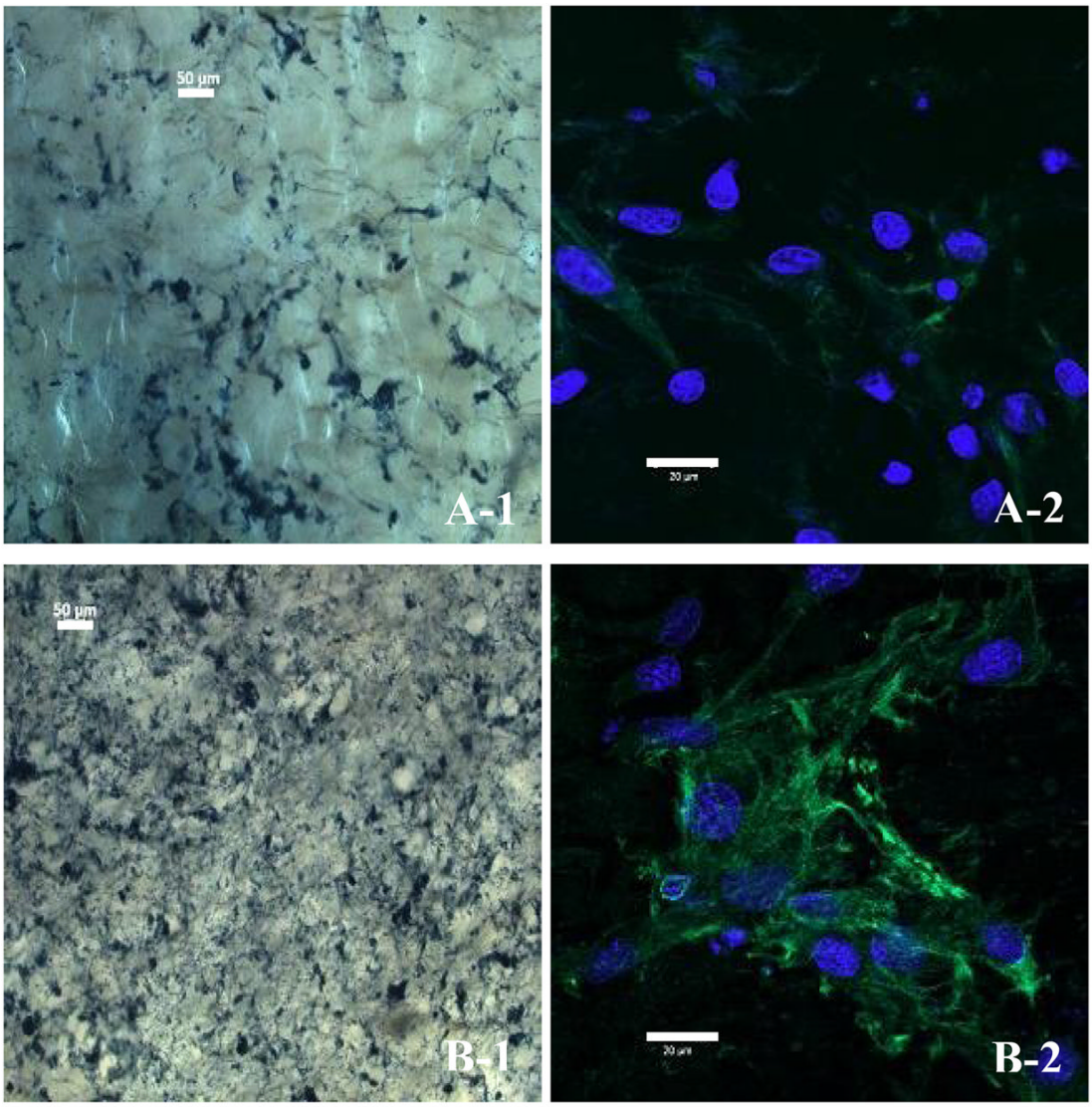

Fig. 4.

Deposition of ECM in collagen matrices. The presence of ECMs are revealed by immunostaining for either elastin expression (dark blue, light microscopy) or fibronectin expression (green, fluorescent microscopy) with cell nuclei stained by DAPI (light blue). Fibroblasts residing in, (A) a glycated collagen matrix, and (B) a non-glycated collagen matrix. Scale bar: 50 μm (A-1, B-1), and 20 μm (A-2, B-2).

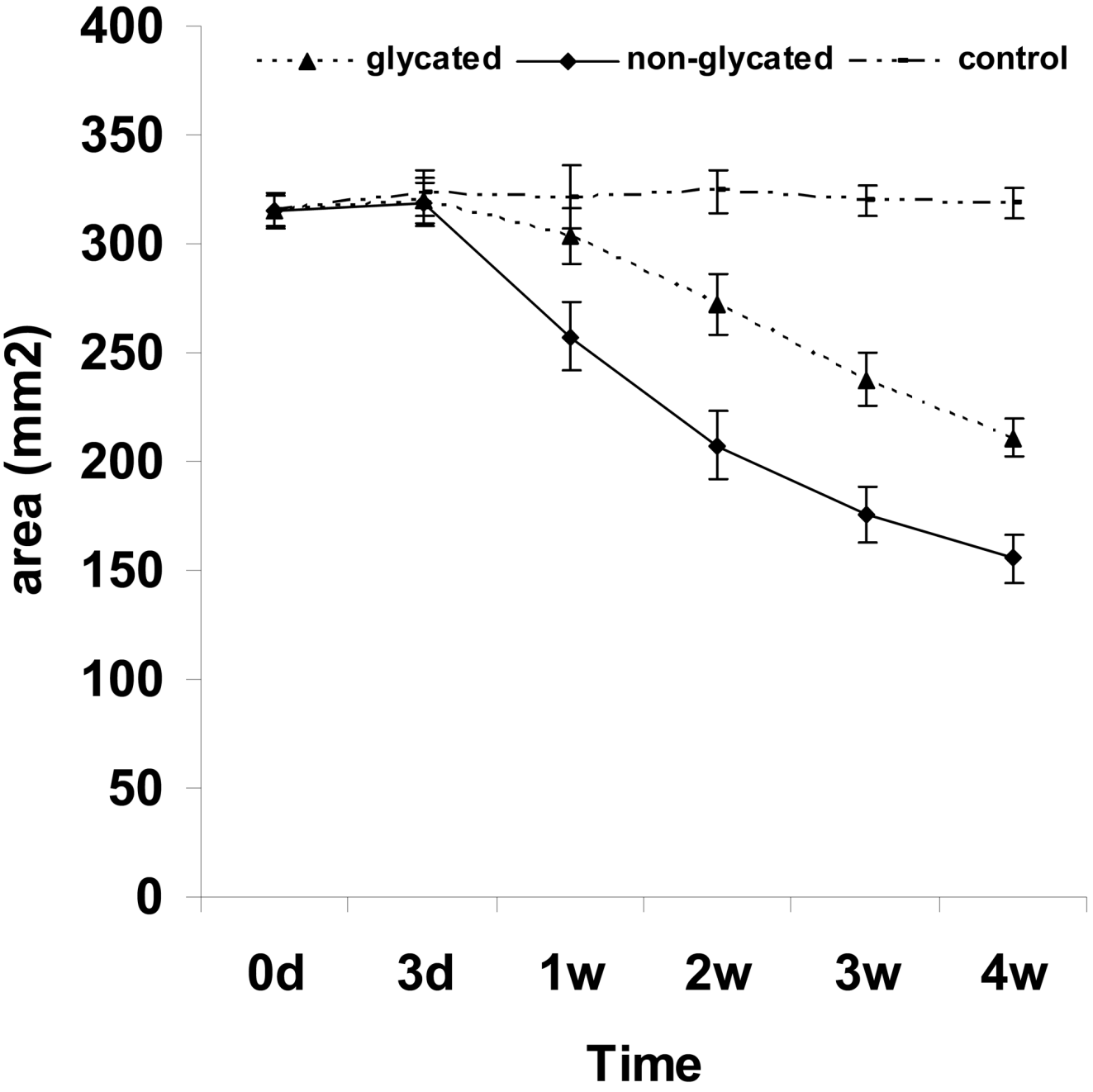

Fig. 5.
Fibroblast mediated contraction of collagen matrices.

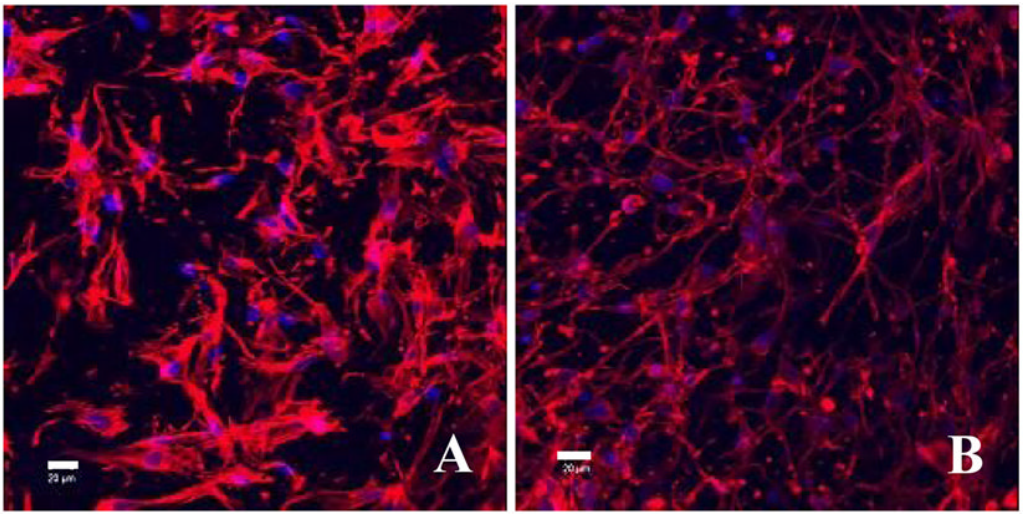

Fig. 6.

Phalloidin stained fibroblasts residing in, (A) a glycated collagen matrix, and (B) a non-glycated collagen matrix; the samples were counterstained by DAPI to reveal cell nuclei (light blue). Scale bar: 20 μm.

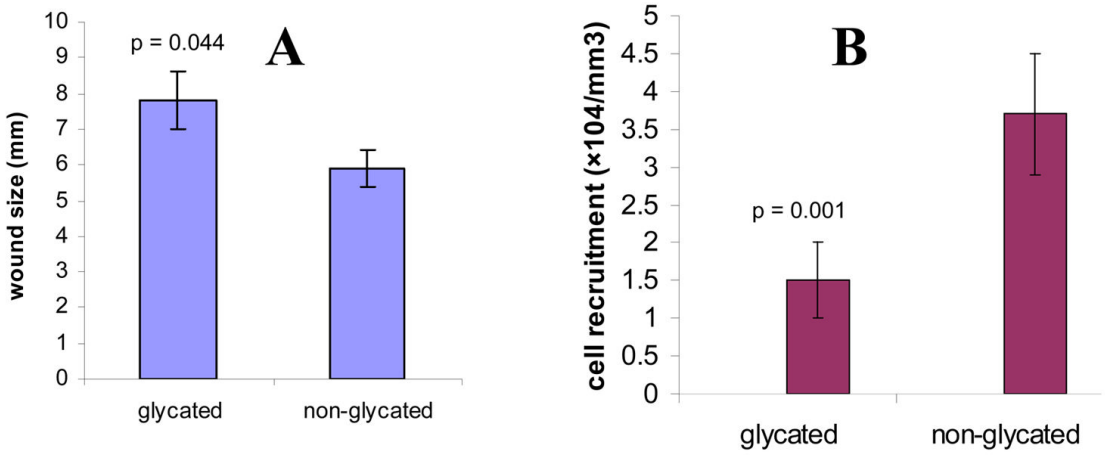

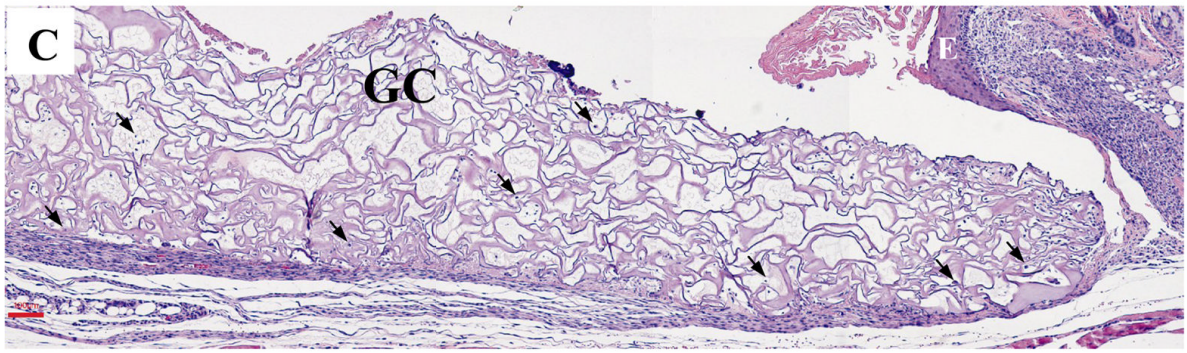

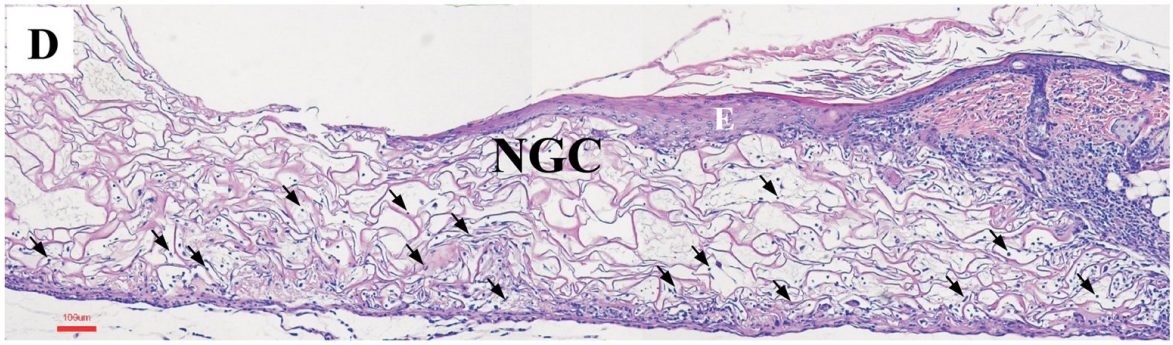

Fig. 7.

Wound healing responses 7 days after implanting collagen matrices (glycated and non-glycated). (A) Comparative wound bed sizes, (B) the extents of cell migration into the interiors of collagen matrices, (C) a typical wound bed implanted with a glycated collagen matrix, GC, and (D) a typical wound bed implanted with a non-glycated collagen matrix, NGC.
E: epidermal hyperplasia/re-epithelialization, and ↟: cells scattered inside the matrices. Scale bar: 100 μm.